Research Article

Artificial neural network models to predict lost circulation in natural and induced fractures

Husam H. Alkinani[1] · Abo Taleb T. Al-Hameedi[1] · Shari Dunn-Norman[1]

Received: 27 April 2020 / Accepted: 3 November 2020 / Published online: 10 November 2020

Abstract
Mud loss is a challenging obstacle in the oil and gas industry. Predicting mud loss can be very useful to stop or prevent this problem. In this study, data of more than 3500 wells collected worldwide were used to create two neural network models to predict mud loss in natural and induced fractures. For both networks, data were separated into three sets: 60% for training, 20% for validation, and 20% for testing. The number of hidden layers and the number of neurons in each hidden layer were optimized after multiple trials. The findings proved that the created models can estimate mud loss for natural and induced fractures within a small error. The overall R^2 for the natural fractures model was 0.956 while the overall R^2 for the induced fractures was 0.925. To further investigate and verify the created networks, both models were tested on 24 new wells (wells not used in the process of constructing the networks). The results indicated the models' predictions closely tract the actual mud loss data with a maximum error of 6.34%. The models have proved their robustness in predicting mud loss and can be used worldwide for mud loss prediction as well as mitigating mud loss by altering the key drilling parameters to prevent or minimize mud loss.

Keywords Artificial neural networks · Machine learning · Mud loss · Lost circulation

1 Introduction

Drilling fluid is a major expense in the oil and gas industry. Drilling fluid performs many functions in rotary drilling. Drilling mud is circulated to remove cuttings and enhance the performance of the drill bit. Cuttings are carried from the borehole to the surface, where cutting will be separated. Furthermore, the following functions are performed by drilling fluid [1]:

1. Minimizing the invasion of the filtrate
2. Decreasing the friction between the sides of the borehole and drill string
3. Sealing permeable formations
4. Maintaining stability for the borehole in uncased sections
5. Limiting reservoir damage
6. Ensuring sufficient formation evaluation
7. Forming a thin, impermeable filter cake that seals pores and reduces the fluid lost into permeable formations.

Drilling mud losses and issues related to lost circulation during drilling the thief zones account for a considerable cost in the oil and gas industry. Millions of dollars are spent annually to stop and minimize this obstacle [2]. Lost circulation can be defined as "the partial or total loss of circulating fluid from the wellbore to the formation. It is the loss of whole fluid, not simply filtrate, to the formation. Losses can result from either natural or induced causes and can range from a couple of barrels per hour to hundreds of barrels in minutes. Lost circulation is one of the drilling's biggest

✉ Husam H. Alkinani, hhappf@umsystem.edu; ✉ Abo Taleb T. Al-Hameedi, ata2q3@umsystem.edu | [1]Missouri University of Science and Technology, 1201 N State St, Rolla, MO 65409, USA.

SN Applied Sciences (2020) 2:1980 | https://doi.org/10.1007/s42452-020-03827-3

expenses in terms of rig time and safety. Uncontrolled lost circulation can result in a dangerous pressure control situation and loss of the well" [3].

Even though it may happen in any zone, some primary factors to loss circulation are high permeability weakly consolidated formations, fracture calcium carbonate reservoirs, and depleted aquifer zones. [4]. Historically, technical journals, papers, manuals, international oil companies training courses, and textbooks have been categorized the types of formations that are highly candidate to have lost circulation problem, and all of them are on the same page in terms of the formation causing lost circulation. These formations are cavernous formations, natural or intrinsic fractures, induced or created fractures, and unconsolidated or highly permeable formations as shown in Fig. 1.

Lost circulation occurrences are classified based on the total amount of mud lost during penetrating thief zones. The amount of mud loss relies on several elements, involving formation characteristics, mud specifications, and fracture gradient. The classifications of mud loss are illustrated as follows, depending on the amount of mud loss [5, 6]:

1. Seepage loss (0.5–1 m^3/hrs or 3–6 bbl/hr): It can happen in most of the penetrated formations, and it is normal during the drilling process due to over-balance drilling phase. Also, it can be named as filtration.
2. Partial loss (1–10 m^3/hrs or 7–70 bbl/hr): this type of mud loss can occur in permeable zones, gravel beds, and small natural and induced fractures.
3. Severe loss (15 m^3/hrs or 95 bbl/hr and above): This type of loss is more complicated and serious than partial loss, and it can lead to complicated consequences.
4. Complete loss: No return from the annulus to the surface will be presented in this kind of mud loss, it is considered the most complicated and serious type of loss since it has many direct and indirect unwanted consequences in the drilling process. This type of mud loss occurs in large natural and induced fractures, vugs, long open sections of gravel, and caverns

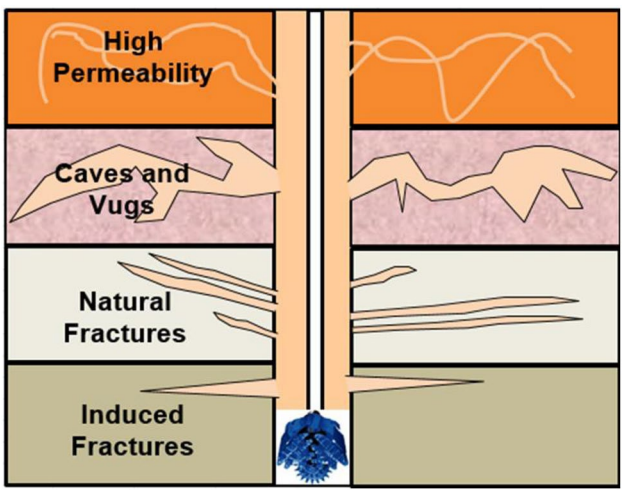

Fig. 1 Candidate formations for lost circulation

Directly or indirectly, lost circulation has many negative impacts on the drilling process, including but not limited to; circulation loss, mechanical and differential stuck pipes, kick, bit damage, etc. [5].

An assessment of the severity of mud loss should be carried before selecting the best lost circulation treatment to be used to stop mud loss. It is distinguished that it is complicated to find one solution to stop lost circulation. Hence, an enormous range of lost circulation treatments are available, including but not limited to, high viscosity pill, fibrous, granular, and flaky materials, and cement slurries. These treatments are classified into generic groups to help in elucidating to recognize their uses. Also, a broad range of plugging materials is available for mitigating lost circulation or restoring circulation during drilling or cementing. Every material or treatment is chosen by relying on the type of mud loss, timing, cost, drilling phase, fluid type, and thief zone. Mud loss treatments and materials are used to accomplish two goals [7, 8]:

1. To bridge across the already existed vugs and fractures.
2. To prohibit the development of new fractures that may be stimulated during the penetration.

The purpose of this paper is to build two neural network models to predict mud loss for natural and induced fractures using data of more than 3500 wells drilled worldwide. This work will eliminate the shortcomings in the literature regarding lost circulation predictions using real-field data collected from various locations around the world.

2 Neural networks

McCulloch and Pitts [9] presented the first neural network research. Rosenblatt [10] developed the perceptron and proved that a perceptron would create a vector

that divides the classes. Rosenblatt [10] believed that structures of more layers can conquer the limitations of a simple perceptron. Nevertheless, there were not any learning algorithms that can determine the weights for a given calculation [11]. A few years after, a network called Adeline was created by Widrow [12]. Minsky and Papert [13] proved that single-layer perceptron cannot solve elementary calculation problems. After that, the neural network's research stopped for 20 years [14]. Then, Hopfield [15] proposed new algorithms, such as back-propagation, that brought life for the neural network's research. Afterward, the neural network applications have gone viral [11]. An artificial neural is a mimic for a biological neuron that can process information. Neurons are the basic building blocks of the nervous system. A typical biological neuron consists of a cell body, an axon, and dendrites. Information in the cell body enters through the dendrites. The cell body then gives an output that travels via the axon then to another receiving neuron, the output from the first neuron becomes an input for the second neuron, and so on.

The human brain has 10–500 billion neurons [16]. The neurons are separated into sections; every section has about 500 neural networks [17]. Every neural network contains about 100,000 neurons where these neurons are linked with thousands of other neurons. This structure is behind the human's complex behavior. A simple task such as moving hands, walking, or catching a cup of coffee requires very complex computations that advanced computers cannot execute, but the human brain can do them. Although computers are faster than human brains (human brain cycle is 10 to 100 milliseconds while computer chips cycle is in nanoseconds), the human brain can still perform much more complex activities than computers due to the sophisticated structures of the neurons [11].

Neural networks are a simulation for the aforementioned biological process. Neural networks are developed based on the following assumptions and mathematical models:

1. Neurons are responsible for processing the information
2. To let the information pass through, the neurons are connected by connection links. Every connection link has weights.
3. To find the output of a neuron after receiving input, an activation function will be applied by the neuron.

The outputs of other neurons are multiplied by the weights of the connection links and enter the neuron. Then, the input data are summed, and the activation function of the neuron is applied which leads to an output. Thus, a neuron can have multiple inputs but only a single output. An artificial neural network has an input layer where the inputs are processed, one or more hidden layers where the feature extraction from the data are processed, and an output layer to process the outputs. Artificial neural networks (ANNs) have been utilized in drilling for a long time. Table 1 shows some applications of ANNs in the drilling industry.

Lost circulation estimation is a limited topic in the literature; only a few papers were published about this topic. Some shortcomings were identified in the previous work as follows [34, 36, 39–42]:

1. Not enough data were used
2. The model is applicable only in a specific area

3 Data and methods

3.1 Data

Figure 2 presents a map with red dots showing the locations where data collected. Many resources were used to collect data such as daily drilling reports (DDR), final well reports, case histories, literature, etc. Two separate databases were created; natural fractures and induced fractures. The data went through processing steps where all outliers, errors, white spaces were removed [43]. Input data were selected based on previous statistical and sensitivity analysis studies conducted that showed the most influential parameters on mud loss as well as experts' opinions [39, 41]. Table 2 shows the parameters used to create the models and a summary of statistics for both induced and natural fractures.

3.2 Data normalization

Normalizing the data is a vital step in the training process for any neural network. Normalization and scaling help simplify the problem being modeled and assist the network in achieving better results [44, 45]. One example of normalizing the data is to make the data range between −1 and 1; this can be obtained using Eq. 1:

$$X_i' = 2\left[\frac{X_i - X_{min}}{X_{max} - X_{min}}\right] - 1$$

Table 1 Applications of ANNs in drilling

Author(s)	Application	Notes
Arehart [18]	Drill bit diagnosis	Used ANNs to find the state of wear of drill bit during drilling
Dashevskiy et al. [19]	Real-time drilling dynamic	Modeling the dynamic behavior of drilling system
Bilgesu et al. [20]	Drill bit selection	Used ANNs to select the "best" bit based on some inputs
Ozbayoglu et al. [21]	Bed height for horizontal wells	Used ANNs to predict bed heights in horizontal or highly inclined wellbores
Vassallo et al. [22]	Bit bounce detection	Used ANNs to detect bit bounce that can be used as a proactive approach to prevent bit whirl and stick–slip
Fruhwirth et al. [23],Wang and Salehi [24]	Drilling hydraulics optimization and prediction	Used ANNs to optimize and predict drilling hydraulics with a practical example
Moran et al. [25],Al-AbdulJabbar et al. [26]	Rate of penetration (ROP) prediction	Used ANNs to predict ROP so that the drill time can be estimated better
Gidh et al. [27]	Bit wear prediction	Used ANNs to predict/ manage bit wear to improve ROP
Lind & Kabirova [28]	Drilling troubles prediction	Used ANNs to forecast problems during the drilling process
Okpo et al. [29]	Wellbore instability	Wellbore stability prediction
Ahmadi et al. [30]	Prediction of mud weight at wellbore conditions	Collected data from the literature
Al-Azani et al. [31] Elkatatny et al. [32],Abdelgawad et al. [33]	Drilling fluid rheological properties	Estimating rheological properties of drilling fluid
Cristofaro et al. [34]	Mud loss	Used multiple artificial intelligence methods to find the best treatment for mud losses
Hoffimann et al. [35]	Drilling reports sentence classifications	Used ANNs to develop a methodology for automating sentences in drilling reports
Li et al. [36]	Lost circulation	Used ANNs to predict lost circulation risk during drilling
Al-AbdulJabbar et al. [37]	Formation top prediction while drilling	Used ANNs to predict formation tops while drilling
Elzenary et al. [38]	Equivalent circulation density (ECD) prediction	Used ANNs to predict ECD while drilling

where $X_i^{'}$ is the normalized value of original value (X_i), X_{min} and X_{max} minimum and maximum values of X_i, respectively [46].

3.3 Activation function

Weight (w) will be assigned to each input, and bias (b) will be assigned for each neuron in the hidden layer. These biases and weights for each input will be summed and will be an input for the activation function. There are several activation functions available in the literature. These activation functions are divided into linear and nonlinear activation functions. Discussion of the activation function is beyond the scope of this paper; details of the activation functions are available in the literature [47]. Hyperbolic tangent sigmoid activation function was selected for the hidden layer while a linear activation function was utilized for the output layer due to its suitability for regression problems [46].

3.4 Feedforward backpropagation

Usually, to create a neural network, data are divided into three sets; training, verification, and testing. This is done to ensure the model's robustness at generalizing to new data. Training data are used in training, verification data are

Table 2 Summary of statistics

Reason	Parameter	Mean	Standard dev	Min	Max
Natural fractures	MW, gm/cc	1.10	0.04	1.04	1.17
	ECD, gm/cc	1.12	0.04	1.06	1.19
	PV, cp	14.10	3.20	6.00	21.00
	Yp, lb/100 ft^2	17.92	3.92	12.00	29.00
	Q, L/Min	2131.43	373.80	1232.00	3168.00
	RPM	79.77	15.78	50.00	120.00
	WOB, Ton	11.85	3.22	4.00	20.00
	Nozzles, TFA, inch^2	3.79	2.24	0.45	10.60
	Actual Loss, m^3/hr	22.73	19.94	0.00	84.00
Induced fractures	MW, gm/cc	1.18	0.06	1.15	2.30
	ECD, gm/cc	1.19	0.07	1.12	2.50
	PV, cp	16.70	3.05	10.00	23.00
	Yp, lb/100 ft^2	15.70	4.56	11.00	30.00
	Q, L/Min	1719.01	274.53	1232.00	2640.00
	RPM	77.01	16.47	55.00	120.00
	WOB, Ton	12.42	3.51	5.00	21.00
	Nozzles,TFA, inch^2	3.35	1.72	0.31	5.96
	Actual loss, m^3/hr	26.35	23.15	0.00	92.00

Fig. 2 Data collection locations

used to verify the model, and testing data are used to test the network and assess the outcomes. Feedforward back-propagation is the process where the data are imported to the model and obtaining a desired output, then the output of the network will be compared with the actual output, the error will backpropagate, and the weights are adjusted until calibration is reached. To prevent overtraining and ensure generalization, the data were divided into 60% for training, 20% for validation, and 20% for testing.

3.5 Network structure

Choosing the number of hidden layers and the number of neurons in the hidden layers is a vital step to create neural networks. There are endless network structures that can be chosen. Choosing too many hidden layers and/or too

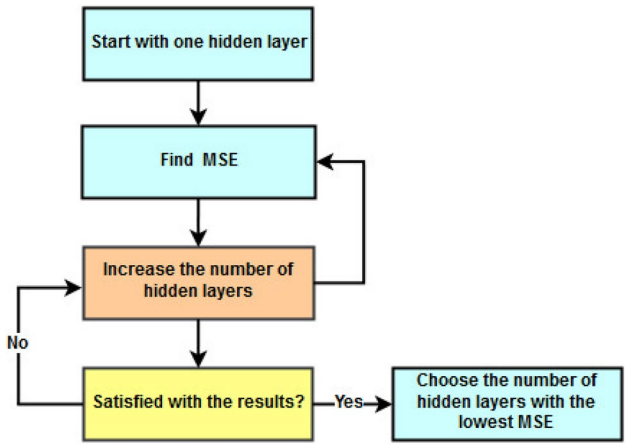

Fig. 3 Process of selecting the optimum number of hidden layers

Table 3 Training algorithms

Description	Acronym
Bayesian Regularization	BR
Conjugate Gradient with Powell/Beale Restarts	CGB
Fletcher–Powell Conjugate Gradient	CGF
Levenberg–Marquardt	LM
One Step Secant	OSS
Polak–Ribiére Conjugate Gradient	CGP
Quasi-Newton	BFG
Resilient Backpropagation	RP
Scaled Conjugate Gradient	SCG
Variable Learning Rate Backpropagation	GDX

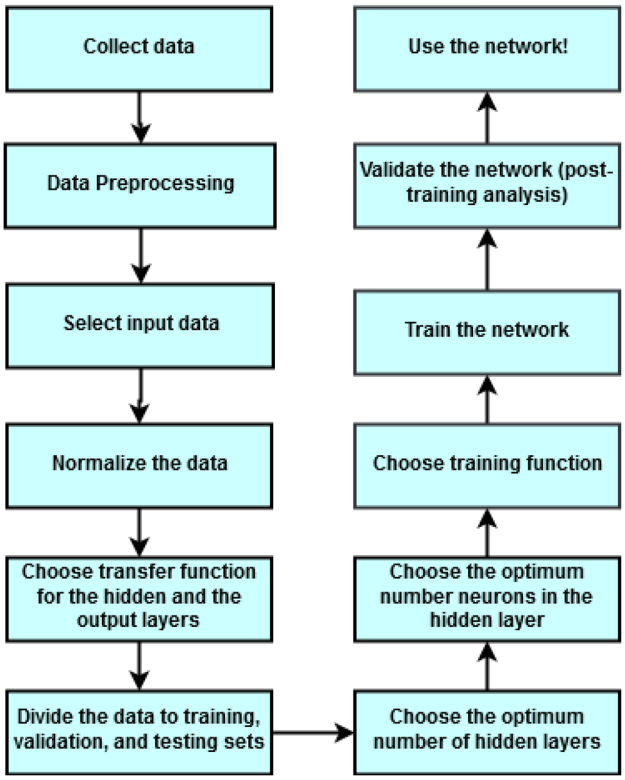

Fig. 4 Summary of the methodology used in this study

many neurons in each hidden layer may result in over-training of the network, meaning the network will lose generalization to new data. Thus, the optimal number of hidden layers and the number of neurons in the hidden layers must be selected. This process was done by trial and error, such that starting with one hidden layer and increasing the number of hidden layers after each trial, the same process was also implemented to select the number of neurons in the hidden layers. Figure 3 summarizes the process of selecting the optimal number of hidden layers. For each trial, the mean square of error (MSE) was calculated, and the scenario with the lowest MSE was selected. MSE was calculated using Eq. 2, where M is the number of data points [46]:

$$MSE = \frac{1}{M}\sum_{i=1}^{M}(Actual - Predicted)^2 \quad (2)$$

3.6 Training algorithms

Table 3 shows a summary of the training algorithms tested in this work. Two criteria were used to select the training algorithms; the algorithm with the lowest MSE and the highest R^2 was selected to train the network. Equation 3 was used to calculate R^2:

$$R^2 = \frac{\sum_{i=1}^{n}\left(\hat{y}_i - \overline{y}\right)^2}{\sum_{i=1}^{n}\left(y_i - \overline{y}\right)^2} \quad (3)$$

where y_i is the actual data point, $\hat{y}_i$ is the estimated data point, and $\overline{y}$ is the average mean of the actual data. Figure 4 summarizes the methodology used in this study.

4 Results and discussion

Since two datasets were collected for the natural and induced fractures, two networks were created: one for the natural and one for induced fractures. The results are divided into natural fractures network results and induced fractures network results.

4.1 Natural fractures network

A neural network with one input layer, one hidden layer with ten neurons, and one output layer was created for the natural fractures dataset. Figures 5 and 6 show the MSE and R^2 for all training functions examined in this study, respectively. LM and BR algorithms have the lowest MSE and the highest R^2 among the other algorithms with the LM algorithms being slightly better than the BR algorithm (LM has lower MSE and higher R^2). Typical BR algorithm does not use validation to stop the network

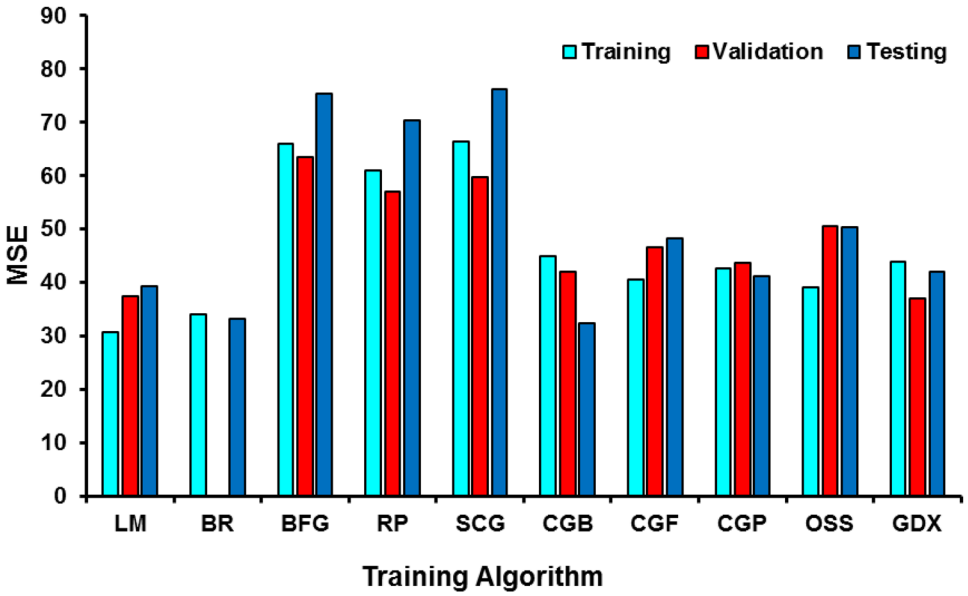

Fig. 5 MSE of all training functions examined in this study (natural fractures)

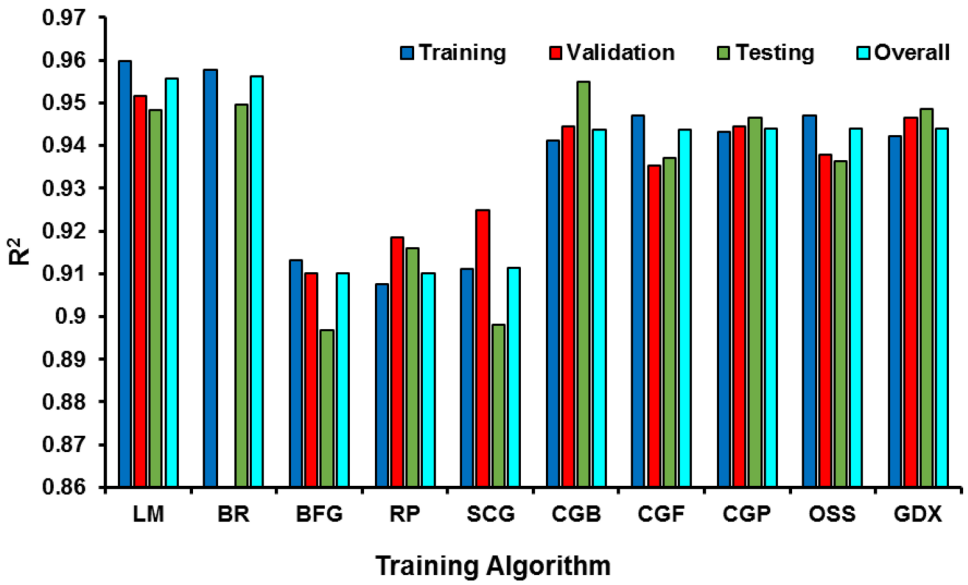

Fig. 6 R^2 of all training functions examined in this study (natural fractures)

when a generalization is reached such that the training can continue until an optimal combination of weights is found. On the other hand, LM usually has the fastest convergence which gives accurate training. Also, the LM normally performs very well in approximation (regression) problems. Training will stop in the LM algorithm when generalization stops improving. Thus, the LM algorithm was chosen to train the network [46].

Figure 7 shows the MSE with iterations for training, validation, and testing sets for the LM algorithm. To avoid overfitting, the MSE in the validation set is monitored and the training will stop once the lowest MSE is reached. Also, testing and validation MSE should have similar characteristics to avoid overfitting and have a rigorous network. Figure 7 shows the training stops after 33 iterations which when the MSE for the validation set is minimum. Moreover, Fig. 7 clearly shows that testing and validation sets have the same MSE characteristics.

Figure 8 shows the actual and predicted mud loss for training Fig. 8a, validation Fig. 8b, testing Fig. 8c, and all

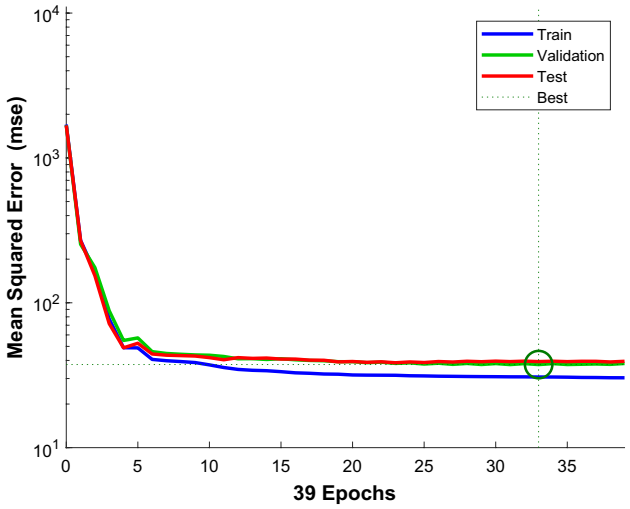

Fig. 7 MSE vs epochs for the LM training function (natural fractures)

Fig. 8d datasets. The R^2 for the training, validation, and testing is 0.96, 0.95, and 0.948, respectively. The network has an overall R^2 of 0.956. With this high R^2, the network can be used to predict mud loss prior to drilling for formations with natural fractures.

Equation 4 can be used to estimate mud loss for formations with natural fractures prior to drilling.

$$MudLoss = \left[\sum_{i=1}^{n} w_{2i}\left(\frac{2}{1+e^{-2\left(\sum_{j=1}^{J} w_{1ij}x_j+b_{1i}\right)}}-1\right)+b_2\right] \quad (4)$$

where n is the number of neurons in the hidden layer that optimized to be ten, w_1 is the hidden layer's weight, w_2 is the output layer's weight, b_1 is the hidden layer's bias, b_2 is the output layer's bias, and x is the input. The j's are related to the input variables such that $j=1$ is MW, $j=2$ is ECD, $j=3$ is PV, $j=4$ is Yp, $j=5$ is Q, $j=6$ is RPM, $j=7$ is WOB, and $j=8$ is Nozzles TFA. Table 4 summarizes the coefficients for Eq. 4.

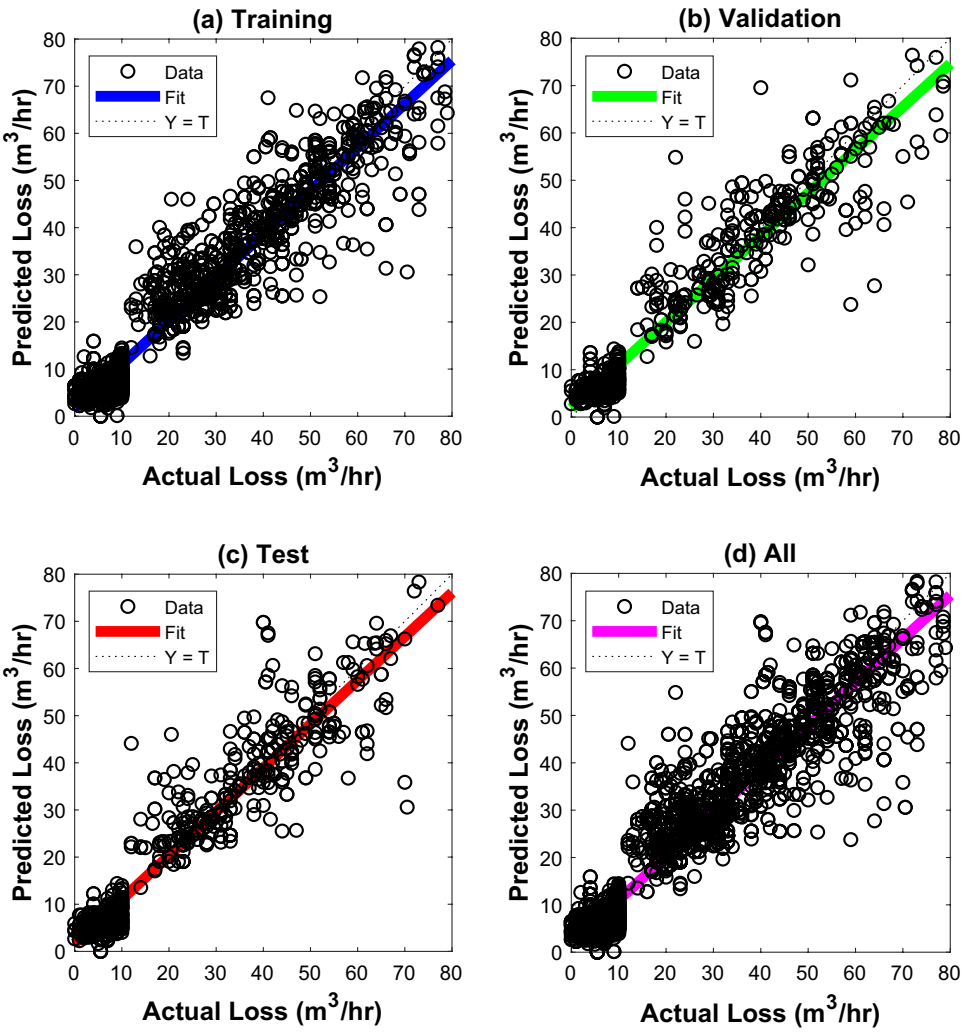

Fig. 8 Predicted and actual mud loss (natural fractures)

Table 4 Coefficients for natural fracture formations mud losses (Eq. (4))

Weights w_{1j}								Hidden layer bias	Weights of output layer	Output layer bias
$j=1$	$j=2$	$j=3$	$j=4$	$j=5$	$j=6$	$j=7$	$j=8$	b_1	w_2	b_2
−2.2091	2.7249	1.8762	0.6220	−0.0617	−1.7078	-0.7524	−1.0397	−1.7124	0.3750	−0.2793
−6.9222	3.2221	2.1353	−1.7348	1.1825	−0.8590	0.6850	2.7215	3.5206	−0.2016	
−0.4195	−0.7027	−4.4217	1.4298	−1.3663	0.2557	4.9967	1.8083	4.1717	0.2147	
5.5710	1.4180	2.3832	0.8779	−0.7672	−0.1834	−1.0082	−0.0979	−4.8003	0.3362	
−2.3232	−3.2751	1.3330	0.5541	−1.0229	0.9844	−0.6204	−2.8423	−0.5922	2.4752	
1.0026	0.1431	−0.1428	1.4370	0.2717	−1.6094	−0.3796	−1.6778	−2.2784	−0.7235	
1.2600	1.0021	2.5369	−0.1617	5.4880	−0.4228	4.0073	−3.1335	−3.9646	0.1092	
3.2746	3.3977	−2.1981	−0.7570	1.8079	−1.2094	1.2321	3.5979	0.6624	1.8705	
3.3066	0.7451	−0.1552	−0.1148	−0.1447	0.5618	0.3344	−0.0443	2.1266	0.6306	
2.3620	−3.3680	−0.4873	−1.0335	−0.3052	1.7558	−1.8901	1.1824	3.5360	−0.5589	

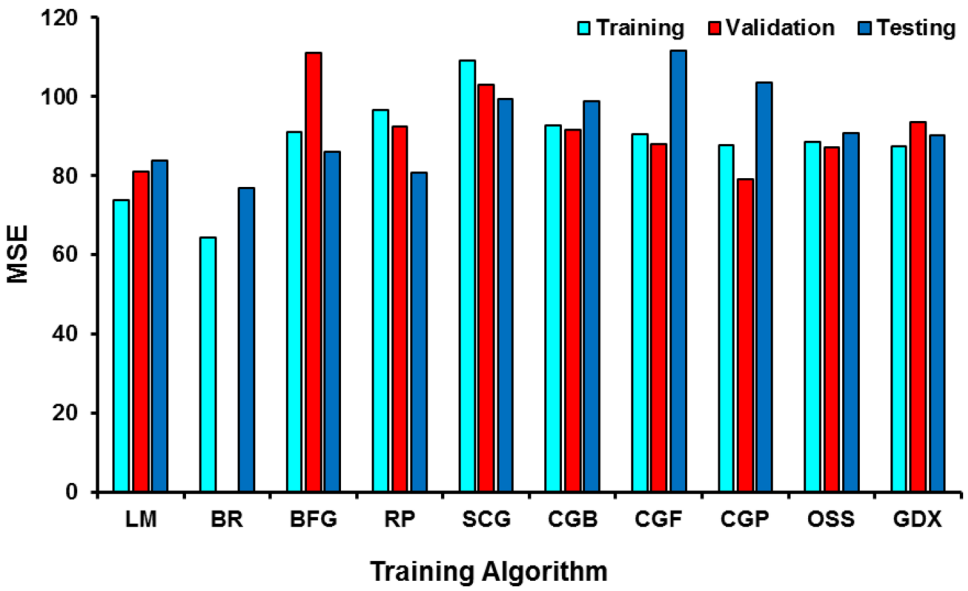

Fig. 9 MSE of all training functions examined in this study (induced fractures)

4.2 Induced fractures network

A neural network with one input layer, one hidden layer with ten neurons, and one output layer was created for the induced fractures dataset. Figures 9 and 10 show MSE and R^2 for all training functions, respectively. Although the BR algorithm has a lower MSE, the LM algorithm was chosen because it has a higher R^2.

Figure 11 shows the MSE for the LM algorithm for training, validation, and testing. Figure 11 shows the training stops after 19 iterations which when the MSE for the validation set is minimum. Moreover, Fig. 11 clearly shows that the testing and validation sets have the same MSE characteristics. Figure 12 shows the actual and predicted mud loss for training Fig. 12a, validation Fig. 12b, testing Fig. 12c, and all Fig. 12d datasets. The R^2 for the training, validation, and testing is 0.928, 0.925, and 0.91, respectively. The network has an overall R^2 of 0.925. With this high R^2, the network can be used to predict mud loss prior to drilling for formations with induced fractures.

Equation 5 can be used to estimate mud loss for formations with induced fractures prior to drilling.

$$MudLoss = \left[\sum_{i=1}^{n} w_{2i}\left(\frac{2}{1+e^{-2\left(\sum_{j=1}^{J} w_{1ij}x_j+b_{1i}\right)}}-1\right)+b_2\right] \quad (5)$$

where n is the number of neurons in the hidden layer that optimized to be ten, w_1 is the hidden layer's weight, w_2 is the output layer's weight, b_1 is the hidden layer's bias, b_2 is the output layer's bias, and x is the input. The j's are related to the input variables such that $j=1$ is MW, $j=2$ is

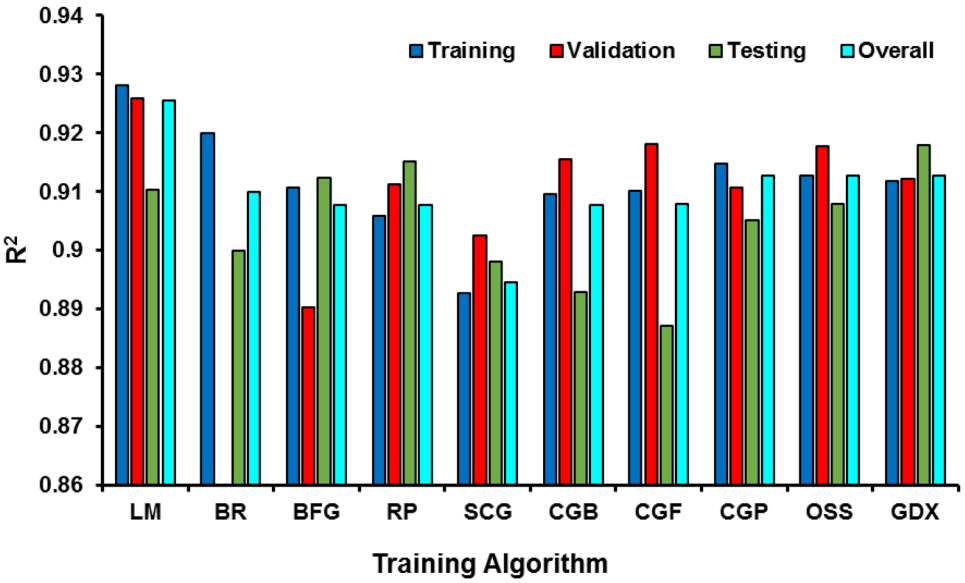

Fig. 10 R^2 of all training functions examined in this study (induced fractures)

ECD, $j=3$ is PV, $j=4$ is Yp, $j=5$ is Q, $j=6$ is RPM, $j=7$ is WOB, and $j=8$ is Nozzles TFA. Table 5 summarizes the coefficients for Eq. 5.

4.3 Verification of the models

To further ensure the validity of the created neural network models, the models were tested on 24 new oil wells from different locations around the world (locations where data were gathered). Table 6 shows the 24 new tested oil wells, 12 wells for naturally fractured formations, and 12 for induced fractured formations. As can be seen, both models closely track the actual mud loss. The highest error in the naturally fractured formations network is about 6.34% in well 3, while the highest error in the induced fractured formations network is about 5.5%. These errors are not significant (one barrel per hour is not significant). Therefore, the networks are reliable to be utilized in the locations where data were collected to estimate mud loss based on key drilling parameters within an acceptable margin of error. Using the created models, key drilling parameters can be set to limit or minimize mud loss and save time and money.

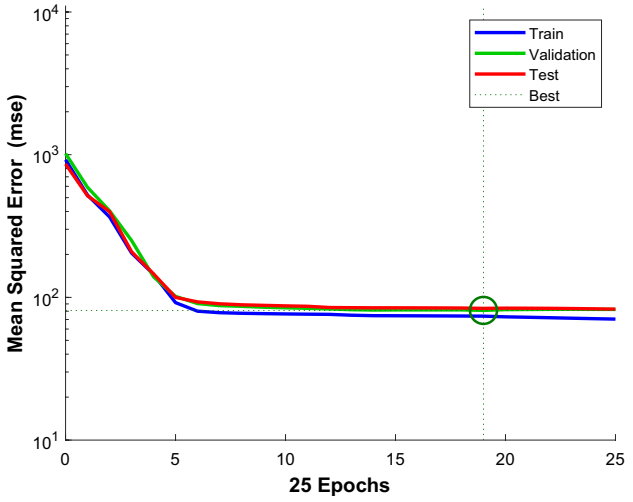

Fig. 11 MSE vs epochs for the LM training function (induced fractures)

5 Conclusion

The following conclusions can be deduced based on this study:

- Two neural networks were created to be used to predict mud loss for natural and induced fractures. The networks showed the ability to predict lost circulations prior to drilling within an acceptable range of error.
- After testing various training algorithms, the LM function was selected to be used to train both networks because it had the highest R^2 which makes it better for predictions.
- The created neural networks can be used in reverse to limit mud loss in induced and natural fractures by setting the key drilling parameters and obtaining a target mud loss.
- To further investigate and verify the created models, 24 new wells were used to test the models. The models' outputs closely tracked the actual mud loss with a maximum error of 6.34%.
- This work overcame the shortcoming in the previous studies about the estimation of mud loss prior to drill-

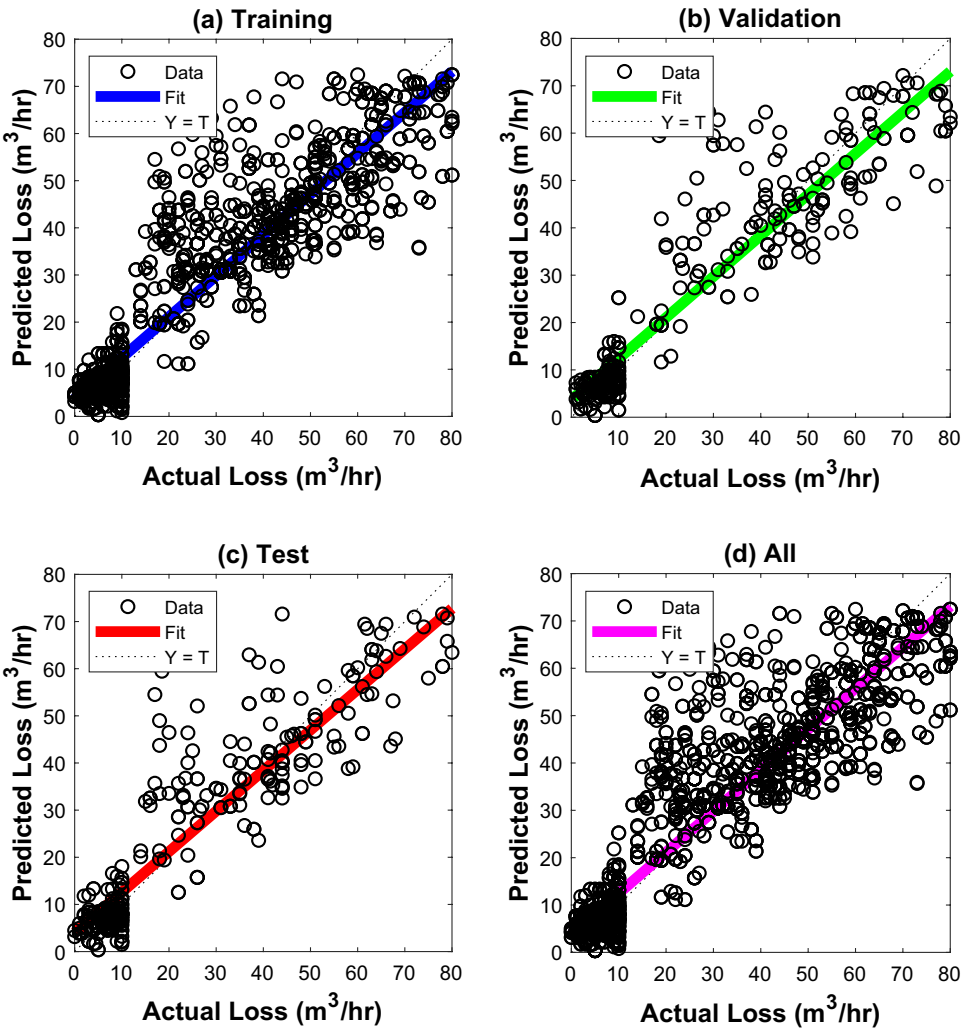

Fig. 12 Predicted and actual mud losses (induced fractures)

Table 5 Coefficients for induced fracture formations mud losses (Eq. (5))

Weights w1j								Hidden layer bias	Weights of output layer	Output layer bias
$j=1$	$j=2$	$j=3$	$j=4$	$j=5$	$j=6$	$j=7$	$j=8$	$b1$	$w2$	$b2$
−0.0188	0.4299	0.5094	−0.1200	−0.4728	0.9857	−2.2359	−1.5879	−0.9569	−0.8401	−0.0934
−1.2088	0.1555	−0.0515	1.6637	−0.4362	0.3206	−1.9913	−0.5783	2.0514	−0.7485	
−1.4972	1.1058	−0.3683	−0.0899	−0.2342	−1.1991	1.8422	1.4864	0.2953	−0.6208	
0.3541	1.3957	0.9587	−2.0335	0.6458	−0.2935	0.9900	1.7517	−0.5481	0.0843	
1.0827	1.4165	4.9306	0.2243	−0.3265	0.6341	−0.3807	1.2828	−0.9051	0.4399	
−0.6141	−0.9271	0.7023	1.8216	−0.1393	−0.0490	−0.5954	−0.9000	−0.5400	0.7831	
−1.0147	−0.5148	−0.2306	1.0537	−2.5582	0.6457	−0.0649	−3.2413	−1.0419	−1.0123	
−0.5832	−0.2497	−2.6341	−0.6176	0.2716	0.5635	0.4701	−0.5470	1.2409	0.5409	
0.5697	0.3100	−0.3131	0.7437	−2.6053	0.4978	−0.1359	−3.0343	0.7000	1.0956	
1.7660	0.2721	−0.6647	4.0852	−0.5448	0.3596	1.3750	1.0492	2.4765	−0.4157	

Table 6 Verifications of the created networks

Natural fractures				Induced fractures			
Well	Actual loss (m^3/hr)	Predicted loss (m^3/hr)	Error (%)	Well	Actual loss (m^3/hr)	Predicted loss (m^3/hr)	Error (%)
1	7	7.13	1.86	13	6.5	6.32	2.74
2	10	10.12	1.20	14	8	7.91	1.15
3	6	6.38	6.34	15	7	7.15	2.10
4	25	26.49	5.97	16	7	7.02	0.35
5	51.5	51.89	0.76	17	10	9.74	2.58
6	31.5	32.43	2.95	18	9	9.28	3.10
7	29	28.76	0.83	19	5	5.28	5.51
8	10	10.11	1.06	20	35	36.79	5.12
9	5	5.01	0.15	21	54	54.71	1.31
10	39	39.89	2.29	22	36	36.56	1.56
11	62	60.47	2.46	23	64	63.81	0.30
12	43	43.91	2.13	24	52	50.36	3.16

ing. This is the first study that provides a generalized model to estimate lost circulation prior to drilling that can be used worldwide.

Acknowledgements The authors would like to thank Basra Oil Company from Iraq for providing us with various realfield data.

Compliance with ethical standards

Conflict of interest There is no conflict of interest.

References

1. Bourgoyne A, Chenevert M, Young FS (1986) Applied Drilling Engineering. Second Edition, SPE Text Book
2. Alkinani HH, Al-Hameedi ATT, Dunn-Norman S, Flori RE, Alsaba MT, Amer AS, Hilgedick SA (2019) Journal of petroleum science and engineering using data mining to stop or mitigate lost circulation. J Pet Sci Eng 173:1097–1108. https://doi.org/10.1016/j.petrol.2018.10.078
3. Baker Hughes Company (1999) Prevention and control of lost circulation best practices
4. Al Menhali S, Kashwani G, Sajwani A (2015) Safety engineering controls of lost circulation during cementing in onshore oil construction projects. This paper Published Online at https://Journal.sapub.orh/ijme. Accessed June 2015
5. Basra oil company. various daily reports, final reports, and tests for 2006, 2007, 2008, 2009 and 2010, 2012, 2013, 2016. Several drilled wells, Basra oil fields, Iraq
6. Nayberg TM, Petty BR (1986) Laboratory study of lost circulation materials for use in oil-base drilling muds. Soc Pet Eng. https://doi.org/10.2118/14995-MS
7. Alkinani HH, Al-Hameedi ATT, Dunn-Norman S, Flori RE, Hilgedick SA, Al-maliki MA, Amer AS (2018) Journal of King Saud University – science examination of the relationship between rate of penetration and mud weight based on unconfined compressive strength of the rock. J King Saud Univ Sci. https://doi.org/10.1016/j.jksus.2018.07.020
8. Jiao D, Sharma MM (1995). Mud-induced formation damage in fractured reservoirs. spe 30107 presented at the European formation damage control conference held in the Hague, the Netherlands, 15–16 May
9. McCulloch WS, Pitts W (1943) A logical calculus of the immanent in nervous activity. Bull Math Biophys 5:115. https://doi.org/10.1007/BF02478259
10. Rosenblatt F (1958) The perceptron: a probabilistic model for information storage and organization in the brain. Psychol Rev 65(6):386–408. https://doi.org/10.1037/h0042519
11. Mohaghegh S (2000) Virtual-intelligence applications in petroleum engineering: part 1—artificial neural networks. Soc Pet Eng. https://doi.org/10.2118/58046-JPT
12. Widrow B (1962) Generalization and information storage in networks of Adaline `Neurons. In: Yovitz MC, Jacobi GT, Goldstein G (eds) Self-organizing systems, symposium proceedings. Spartan Books, Washington, DC, pp 435–461
13. Minsky M, Papert S (1969) Perceptrons. an introduction to computational geometry. MIT press, Cambridge, MA
14. Hertz J, Krogh A, Palmer RG (1991) Introduction to the theory of neural computation. Reading. Addison-Wesley, California
15. Hopfield, J. (1982). Neural networks and physical systems with emergent collective computational abilities. Proceedings of the national academy of sciences of the United States of America. https://www.jstor.org/stable/12175, vol 79, No 8, pp 2554–2558
16. Rumelhart DE, McClelland JL (1986) Parallel distributed processing: Explorations in the microstructure of cognition: Foundations, vol 1. The Mit Press, Cambridge, Massachusetts
17. Stubbs D (1988) Neurocomputers. MD Comput 5(3):14–53
18. Arehart RA (1990) Drill-bit diagnosis with neural networks. Soc Pet Eng. https://doi.org/10.2118/19558-PA
19. Dashevskiy D, Dubinsky V, Macpherson JD (1999) Application of neural networks for predictive control in drilling dynamics. Soc Pet Eng. https://doi.org/10.2118/56442-MS
20. Bilgesu HI, Al-Rashidi AF, Aminian K, Ameri S (2001) An unconventional approach for drill-bit selection. Soc Pet Eng. https://doi.org/10.2118/68089-MS
21. Ozbayoglu EM, Miska SZ, Reed T, Takach N (2002) Analysis of bed height in horizontal and highly-inclined wellbores by using artificial neural networks. Soc Pet Eng. https://doi.org/10.2118/78939-MS
22. Vassallo M, Bernasconi G, Rampa V (2004) Bit bounce detection using neural networks. Society of Exploration Geophysicists, US

23. Fruhwirth RK, Thonhauser G, Mathis W (2006) Hybrid simulation using neural networks to predict drilling hydraulics in real time. Soc Pet Eng. https://doi.org/10.2118/103217-MS
24. Wang Y, Salehi S (2015) Drilling hydraulics optimization using neural networks. Society of Petroleum Engineers. https://doi.org/10.2118/173420-MS
25. Moran DP, Ibrahim HF, Purwanto A, Osmond J (2010) Sophisticated ROP prediction technology based on neural network delivers accurate drill time results. Soc Pet Eng. https://doi.org/10.2118/132010-MS
26. Al-AbdulJabbar A, Elkatatny S, Mahmoud M, Abdulraheem A (2018a) Predicting rate of penetration using artificial intelligence techniques. Soc Pet Eng. https://doi.org/10.2118/192343-MS
27. Gidh YK, Purwanto A, Ibrahim H (2012) Artificial neural network drilling parameter optimization system improves rop by predicting/managing bit wear. Soc Pet Eng. https://doi.org/10.2118/149801-MS
28. Lind YB, Kabirova AR (2014) Artificial neural networks in drilling troubles prediction. Soc Pet Eng. https://doi.org/10.2118/171274-MS
29. Okpo EE, Dosunmu A, Odagme BS (2016) Artificial neural network model for predicting wellbore instability. Soc Pet Eng. https://doi.org/10.2118/184371-MS
30. Ahmadi MA, Shadizadeh SR, Shah K, Bahadori A (2018) An accurate model to predict drilling fluid density at wellbore conditions. Egypt J Pet 27(1):1–10. https://doi.org/10.1016/j.ejpe.2016.12.002
31. Al-Azani K, Elkatatny S, Abdulraheem A, Mahmoud M, Al-Shehri D (2018) Real time prediction of the rheological properties of oil-based drilling fluids using artificial neural networks. Soc Pet Eng. https://doi.org/10.2118/192199-MS
32. Elkatatny S, Tariq Z, Mahmoud M (2016) Real time prediction of drilling fluid rheological properties using artificial neural networks visible mathematical model (white box). J Pet Sci Eng 146:1202–1210. https://doi.org/10.1016/j.petrol.2016.08.021
33. Abdelgawad K, Elkatatny S, Mousa T, Mahmoud M, Patil S (2018) Real time determination of rheological properties of spud drilling fluids using a hybrid artificial intelligence technique. Soc Pet Eng. https://doi.org/10.2118/192257-MS
34. Leite Cristofaro RA, Longhin GA, Waldmann AA, de Sá CHM, Vadinal RB, Gonzaga KA, Martins AL (2017) Artificial intelligence strategy minimizes lost circulation non-productive time in brazilian deep water pre-salt. Offshore Technol Conf. https://doi.org/10.4043/28034-MS
35. Hoffimann J, Mao Y, Wesley A, Taylor A (2018) Sequence mining and pattern analysis in drilling reports with deep natural language processing. Soc Pet Eng. https://doi.org/10.2118/191505-MS
36. Li Z, Chen M, Jin Y, Lu Y, Wang H, Geng Z, Wei S (2018) Study on intelligent prediction for risk level of lost circulation while drilling based on machine learning. American Rock Mechanics Association, Alexandria
37. Al-AbdulJabbar A, Elkatatny S, Mahmoud M, Abdulraheem A (2018b) Predicting formation tops while drilling using artificial intelligence. Soc Pet Eng. https://doi.org/10.2118/192345-MS
38. Elzenary M, Elkatatny S, Abdelgawad KZ, Abdulraheem A, Mahmoud M, Al-Shehri D (2018) New technology to evaluate equivalent circulating density while drilling using artificial intelligence. Soc Pet Eng. https://doi.org/10.2118/192282-MS
39. Al-Hameedi AT, Dunn-Norman S, Alkinani HH, Flori RE, Hilgedick SA (2017) Limiting drilling parameters to control mud losses in the dammam formation, south Rumaila field. American Rock Mechanics Association, Iraq
40. Al-Hameedi AT, Dunn-Norman S, Alkinani HH, Flori RE, Hilgedick SA (2017). Limiting drilling parameters to control mud losses in the shuaiba formation, south Rumaila field, Iraq. Paper presented at AADE National Technical Conference on Paper AADE-17- NTCE- 45, 2017, Houston, Texas, www.AADE.org. Accessed 11–12 Apr 2017
41. Al-Hameedi ATT, Alkinani HH, Dunn-Norman S, Flori RE, Hilgedick SA, Amer AS, Alsaba MT (2018) Using machine learning to predict lost circulation in the Rumaila field, Iraq. Soc Pet Eng. https://doi.org/10.2118/191933-MS
42. Al-Hameedi ATT, Alkinani HH, Dunn-Norman S, Flori RE, Hilgedick SA, Alkhamis MM, Alsaba MT (2018) Predictive data mining techniques for mud losses mitigation. Soc Pet Eng. https://doi.org/10.2118/192182-MS
43. Alkinani HH, Al-Hameedi AT, Flori RE, Dunn-Norman S, Hilgedick SA, Alsaba MT (2018) Updated classification of lost circulation treatments and materials with an integrated analysis and their applications. Soc Pet Eng. https://doi.org/10.2118/190118-MS
44. Saeedi A, Camarda KV, Liang J-T (2007) Using neural networks for candidate selection and well performance prediction in water-shutoff treatments using polymer gels - a field-case study. Soc Pet Eng. https://doi.org/10.2118/101028-PA
45. Zabihi R, Schaffie M, Nezamabadi-pour H, Ranjbar M (2011) Artificial neural network for permeability damage prediction due to sulfate scaling. J Pet Sci Eng 78(3–4):575–581. https://doi.org/10.1016/j.petrol.2011.08.007
46. Demuth H, Beale M, Hagan M (2007) Neural network toolbox 5 user's guide. The MathWorks Inc., USA
47. Feng J, Lu S (2019) Performance analysis of various activation functions in artificial neural networks. J Phys Conf Ser 1237:022030. https://doi.org/10.1088/1742-6596/1237/2/022030